British Journal of Medicine & Medical Research
4(4): 937-948, 2014

SCIENCEDOMAIN *international*
www.sciencedomain.org

Measuring Cranial Soft Tissue Thickness with MRI or Force-Compensated Tracked Ultrasound

Floris Ernst[1*], Ralf Bruder[1], Tobias Wissel[1,2], Patrick Stüber[1,2] and Achim Schweikard[1]

[1]Institute for Robotics and Cognitive Systems, University of Lübeck Ratzeburger Allee 160, 23562 Lübeck, Germany.
[2]Graduate School for Computing in Medicine and Life Sciences, University of Lübeck Ratzeburger Allee 160, 23562 Lübeck, Germany.

Authors' contributions

Authors FE and AS designed the study, evaluated the data and wrote the manuscript. Author TW performed the data extraction and segmentation. Author PS managed the hardware setup. Author RB coordinated the experiments. All authors read and approved the final manuscript.

Original Research Article

Received 11th September 2013
Accepted 1st October 2013
Published 28th October 2013

ABSTRACT

Aims: A new approach to patient tracking in cranial stereotactic radiosurgery relies on contact-free localisation of the cranial bone. It requires accurate information about the soft tissue thickness on the patient's forehead, which in this work is measured using two independent modalities: magnetic resonance imaging (MRI) and force-compensated tracked ultrasound.
Methodology: High resolution MRI scans and ultrasound data of the forehead were recorded and the soft tissue thickness was extracted. The datasets were registered using the iterative closest point algorithm with high accuracy (RMS error < 0.5 mm after artefacts from data acquisition were removed). Tissue deformation was analysed using a robotic setup with force control where the ultrasound transducer was pressed against the skin.
Results: The force compensation setup showed that a tissue compression factor of 0.75 can be assumed for typically applied forces of 7-10N. This factor was confirmed by comparing histograms of soft tissue thickness. Comparing soft tissue thickness as measured by MRI and ultrasound showed a mean error of 0.14mm and a standard

**Corresponding author: Email: ernst@rob.uni-luebeck.de*

deviation of 0.87mm.
Conclusion: We could show that, using MRI as a ground truth, data from 2D ultrasound can be compensated for pressure and can also be used to generate realistic values of soft tissue thickness.

Keywords: Cranial radiotherapy; force-compensated ultrasound; soft tissue thickness; motion management.

1. INTRODUCTION

In stereotactic cranial radiosurgery, it is vital to ensure that the location of the radiation target does not move or, if it does, is known in real time. In typically used clinical systems, some way of fixation is used, either with thermoplastic masks, additional bite blocks or dental plates, or stereotactic frames [1,2]. While thermoplastic masks are the most comfortable form of fixation, they also are the least reliable: inter-fraction motion of more than 2 mm and intra-fraction motion of up to 1.1 mm have been reported [3,4]. In contrast, stereotactic frames have been shown to be much more reliable, with inter-fraction errors below 0.8 mm [5].

We are currently developing a system for contact-free localisation of the human skull [6]. This system makes use of infrared light to measure features of the soft tissue on the patient's forehead. It is envisioned to use these features and information about the thickness of the soft tissue on the patient's forehead to compensate for this tissue and allow for direct tracking of the cortical bone. This technology, however, has to model the functional relationship between optically recorded skin features and a ground truth of tissue thickness. This modelling needs to be done for each patient individually and thus requires accurate tissue thickness measurements.

To determine the ground truth of soft tissue thickness on the human skull, we have used high-resolution magnetic resonance imaging (MRI) scans. Since this type of data may not always be available (it needs a three Tesla MRI scanner), we evaluate a different approach using 2D ultrasound. If it is possible to compensate for contact pressure, it will be a realistic and readily available alternative.

2. MATERIAL AND METHODS

Due to its non-invasiveness and high precision, we recorded MR images using T1 weighting from a male test subject. The images were acquired in a 3D k-space by applying phase coding for the in-plane positions and frequency coding in slice direction. Using a 3D region-of-interest (ROI) of 240 mm × 240 mm × 90 mm (1600 × 1600 × 90 voxels) at the forehead this measurement sequence is capable of quickly acquiring a highly resolved volume (reconstructed resolution of 0.15 mm × 0.15 mm × 1 mm). The ROI was aligned to the anterior commissure – posterior commissure line (AC-PC line) of the subject to set one of the coordinate axes of the volume orthogonal to the forehead.

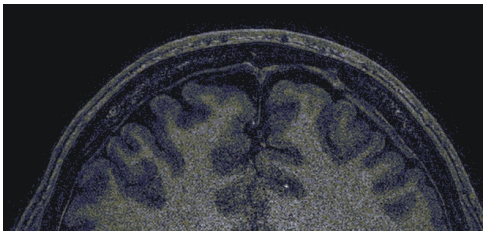

(a) Typical MR slice as recorded in our first experiment, clearly showing the cortical bone and skin surfaces.

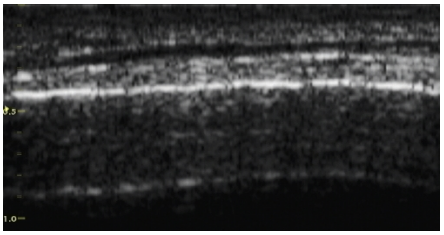

(b) Typical ultrasound scan as recorded during the first ultrasound experiment. Depth is shown in yellow [cm].

Fig. 1. Data recorded using MRI (left) and tracked ultrasound (right)

Due to the T1 weighting, skin and fat are corresponding to high intensities (bright) and bone or liquid to low intensities (dark) in the MRI scan (see Fig. 1(a)). Additionally, the same test person was subjected to two experimental setups for acquiring ultrasound scans. First, we collected tissue ultrasound samples with an optically tracked 2D ultrasound probe (see Fig. 2(a)). The optical marker was calibrated such that the position reported by the tracking system was centred on the bottom of the probe, i.e. in direct contact with the skin. The orientation of the recorded pose matrix was aligned with the ultrasound plane: the *z*-axis in beam direction and the *x*-axis perpendicular to the beam direction. Consequently, it was possible to reconstruct the position of the probe on the subject's forehead. Simultaneously, the position of a bite block marker was recorded to compensate for head motion. The data collected was then processed to extract the soft tissue thickness. A typical ultrasound scan is shown in Fig. 1(b). Due to visibility constraints of the tracking system, the forehead was scanned in two parts (separate scans for the right and left parts of the forehead).

Ultrasound data was acquired with a Vivid 7 Dimension ultrasound station by GE Healthcare using an i13L 2D probe. Optical tracking was performed using a Polaris Spectra system (Northern Digital, Inc.).

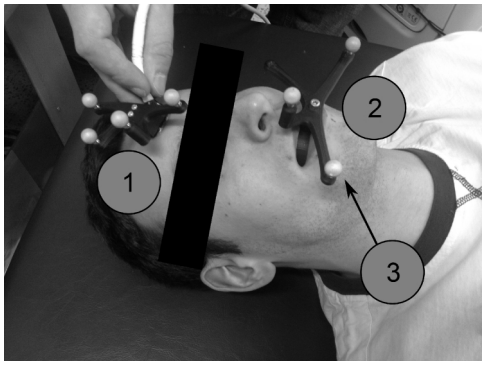

(a) Setup for collecting tracked 2D ultrasound data. The probe (1) and bite block (2) are equipped with marker spheres (3) which can be tracked by an optical tracking system.

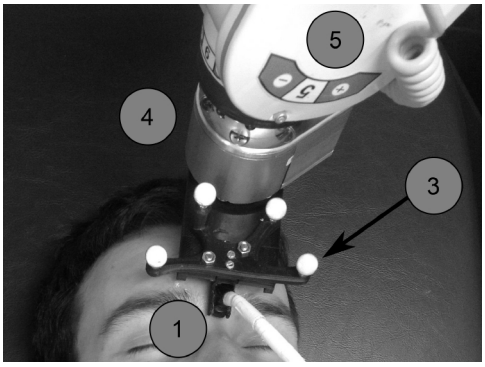

(b) Setup for determining the influence of force on the soft tissue thickness, showing the ultrasound probe (1), marker spheres (3), the force-torque sensor (4) and the robot (5).

Fig. 2. Setup for the ultrasound experiments.

Fig. 1(b) clearly shows the bone surfaces (bright white line at a depth of about 4.5 mm), the inner surface of the bone (lowest edge, with medium echogenicity at a depth of about 9 mm) and the different layers of skin and muscles. To determine the thickness of the soft tissue, the cortical bone's surface was extracted in the centre of the image. This was done semi-automatically.

In a second experiment, the ultrasound transducer was attached to a custom-built force-torque sensor assembly [7] which, in turn, was mounted to an industrial robot (Adept Viper s850), see Fig. 2(b). The robot was setup such that the probe could be pressed against the subject's forehead with a defined force (up to 25 N). Using this setup, it was possible to simultaneously record ultrasound images as well as the force exerted by the robot, allowing us to determine the influence of force on the measured thickness of the soft tissue.

2.1 Soft Tissue Estimation using MRI Scans

2.1.1 Segmentation

After restricting the MR volume to the subject's forehead, the skin and bone surface have been extracted in four main steps shown in Fig. 3. First, a subject-specific intensity threshold was applied to the smoothed volume. This smoothing was achieved by a Gaussian low pass filter and cuts off noise in higher spatial frequency ranges (see Fig. 3(b)). After binarizing, opening and closing operators merged sub regions in the images to obtain more compact main regions (see Fig. 3(c)). These morphological operators were applied several times using disk-shaped structural elements of different sizes. Third, a region-growing algorithm was used to select and finally extract the skin region from the image (see Fig. 3(d)). Finally, the Canny algorithm was used to find the edges corresponding to the skin and bone surfaces irrespectively of their orientation (see Fig. 3(e)).

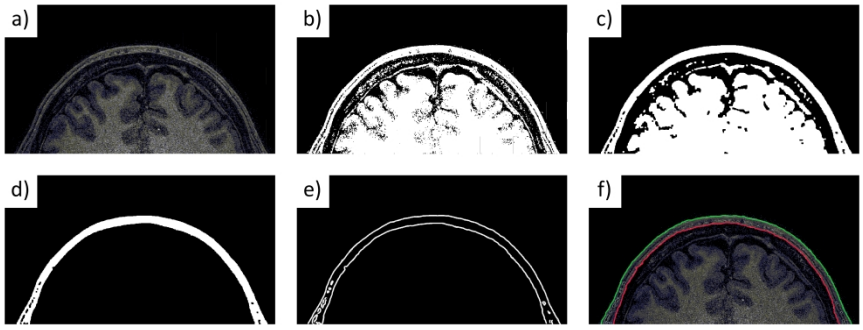

Fig. 3. Segmentation pipeline (from top left to bottom right): (a) raw MRI slice (ROI extracted from the forehead), before applying: (b) image binarization, (c) morphological operators, (d) region growing and (e) Canny edge detection, (f) original image overlaid with segmentation result (green: skin, red: bone).

The last part of the segmentation pipeline has been kept in a semi-automated manner to allow for manual corrections possibly necessary to compensate for rare artefacts caused by blood vessels or muscles within the tissue. Fig. 3(f) illustrates the original image overlaid with the skin (green) and bone (red) surfaces.

2.1.2 Skin Extraction

Using the segmentation output, point clouds in 3D space were generated in order to extract the thickness information for each location on the skin surface. To guarantee stable surface interpolation, the point cloud was decomposed into three patches that were rotated in space to align their main principal component parallel to the *x*-*y*-plane. After interpolating, surface normal vectors to tangential planes in each surface location were computed.

The soft tissue thickness was then obtained as the distance from each location on the skin surface to the penetration point on the bone surface taken along the normal directions.

2.2 Soft Tissue Estimation using Ultrasound

2.2.1 Skin and Bone Surface Extraction

The images obtained from the ultrasound station were segmented semi-automatically: the cranial bone was detected in the centre of the images using an intensity search, which was manually confirmed for each image. This position in image space was converted to a distance value d_i using the distance information of the ultrasound machine. Since each ultrasound measurement was accompanied by pose matrices describing the positions of the transducer and the bite block, the position of the skin's surface corresponding to the ultrasound probe's position was computed by offsetting the ultrasound probe's pose matrix by the bite block's pose matrix to compensate for head motion. Then the corresponding position on the cranial bone was obtained by multiplying the resulting pose matrix with $(0,0,-d_i,1)^T$. The resulting point clouds were used to generate interpolated surfaces of the skin and underlying bone.

2.2.2 Tissue Thickness Estimation

In a procedure similar to the one used on the MR data, the thickness of the soft tissue was estimated by casting rays for each point in the surface point cloud towards the bone point cloud. The distance between the surface point and the closest patch of the bone surface was used as soft tissue thickness at this point. Note that this procedure is necessary because the thickness values d_i obtained from the ultrasound data are not necessarily measured perpendicularly to the skin surface. We could not use the same approach as for the MR data (using skin surface normals) due to the small amount of skin surface samples.

2.2.3 Estimation of Compression Factors

As outlined above, it is necessary to determine the influence of transducer force on the measured soft tissue thickness. It is clear that it is not possible to perform ultrasound measurements without applying force, so the compression effects need to be analysed. This has been done using the robotic setup described before. The robot was moved in a direction perpendicular to the skin surface at 0.1% of its maximum speed. The force along this axis was continuously recorded. Once the transducer came in contact with the tissue, ultrasound images were recorded and the distance to the cortical bone was extracted. Using this approach, it was possible to determine the amount of tissue compression as a function of applied force.

Additionally, all computations were based on the assumption of a typical ultrasound contact force in the range of 7-10 N, which was established from the perception of three test persons undergoing ultrasound acquisition in a clinical setting.

2.3 Registration of MR and Ultrasound Surfaces

As a final step, the skin surfaces from the MR data and the ultrasound data were registered to compare the depth maps recorded. Registration was performed using an iterative closest point algorithm (ICP) [8,9] in a two-step approach. First, to ensure good point-to-point correspondences, the MRI data cloud was interpolated to a uniform resolution of 0.15 mm. Then the complete data sets were matched and all points with a registration error of more than 0.75 mm were removed. In a second step, the ICP algorithm was run again. The transformation matrix obtained in the second run was then applied to all points in the dataset, including those removed after the first run. Then all samples with registration errors of more than 1 mm were assumed to be outliers and were removed from the final dataset.

3. RESULTS AND DISCUSSION

3.1 Extracted Surfaces and Thickness Maps

3.1.1 MRI data

Using the approach described in Section 2.1, it was possible to successfully segment skin and bone surfaces from the MRI data. Fig. 4(a) illustrates the surfaces of the cortical bone (red) and the skin (green) as well as the normal vectors (blue) to the skin surface.

The resulting soft tissue is shown as a thickness map in Fig. 4(b). Higher values were mainly found above the eyes and at both temporals. Furthermore, the v-shaped structure above the eyebrows presumably constitutes muscles lying underneath the skin.

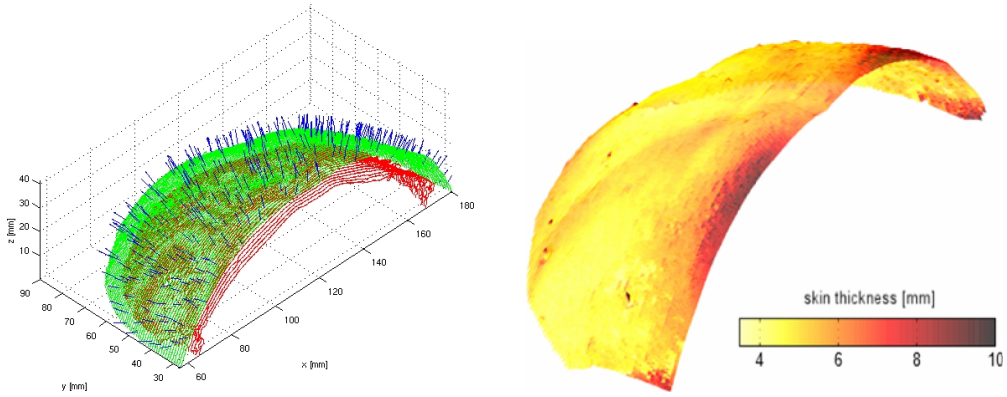

(a) Normal vectors on skin surface from MRI data (b) Computed soft tissue thickness from MRI data

Fig. 4. Left. Soft tissue thickness is obtained by casting vectors perpendicular to the skin surface (green) towards the cranial bone (red). Right: The resulting distance overlaid as a colormap is plotted with the 3D surface of the forehead.

3.1.2 Ultrasound Data

Similarly, the approach using the ultrasound data resulted in the generation of two surfaces. Note that, due to visibility constraints of the tracking system, the surface was sampled in two passes between which the subject had to rotate his head, resulting in an overlap at the centre of the forehead. The area around the temporals is also subject to measurement errors which, however, do not result from overlap but from poor visibility of the optical markers on the ultrasound probe.

Using the approach described in Section 2.2, a thickness map was derived. It is shown in Fig. 5. Here, the artefacts arising from two-batch acquisition can be seen: in the centre of the forehead, the skin surface is not smooth but somewhat jagged.

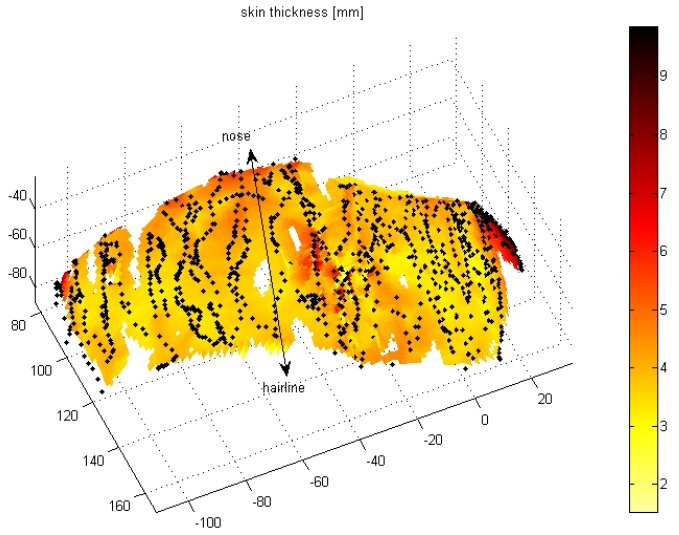

Fig. 5. Soft tissue thickness in mm as extracted from ultrasound. Black dots are positions of the ultrasound probe, the colour is indicative of the measured soft tissue thickness. Note the presence of artefacts in the central area and around the temporals.

3.1.3 ICP Registration

As described before, the skin surfaces from ultrasound and MRI were registered using the ICP algorithm. The initial dataset comprised 1012 samples of ultrasound data. The first ICP registration converged with a root mean square (RMS) error of 1.797 mm. For the second run, 423 samples (with error > 0.75 mm) were removed. The second iteration converged with an RMS error of 0.4686 mm. Then the transformation matrix of the second run was applied to all 1012 samples. The transformed full data set was subject to outlier identification (points with an error of more than 1 mm), which showed 320 points to be off. Removing these points reduced the registration RMS error to 0.456 mm on 692 samples. The result of the registration is shown in Fig. 6.

3.2 Force Compensation

Our experiment showed that soft tissue thickness is directly related to the force. Measurements at different positions on the forehead showed that a significant change of the soft tissue thickness is caused by a force which measures up to 7 N. A stronger force did not result in a significant modification of the thickness since the tissue reached a maximum level of compression. Fig. 7 shows the results of one experiment. Note that it was already possible to measure soft tissue thickness before contact to the skin and after contact with the skin was lost. This effect is caused by ultrasound gel filling the gap between transducer and the subject's skin surface.

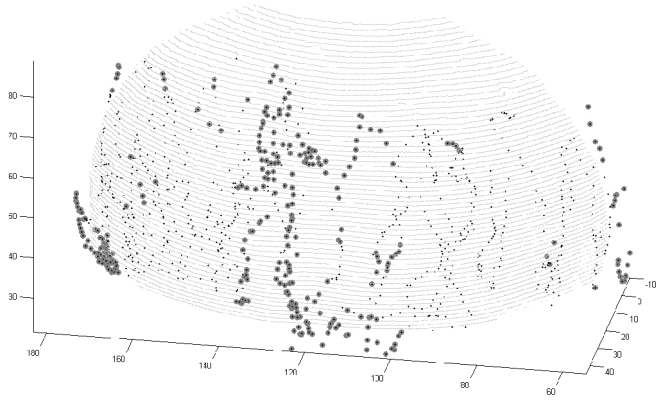

Fig. 6. Results of the ICP registration. MRI data is shown in light grey, ultrasound data is shown in black. Outliers (points with a registration error of more than 1 mm) are marked with dark grey. Note how these points are predominantly either outside the MR data, at the temporals or at the centre of the forehead where artefacts from overlapping and poor visibility occurred.

From this data, it is reasonable to assume an approximate compression factor of 0.77 for typical ultrasound contact force (between 7 and 10 N). More specifically, this can be computed from Fig. 7: the first contact between the ultrasound probe and the forehead results in a tissue thickness reading of 4.15 mm. Next, it is shown that the tissue is compressed to a mean value of 3.17 mm (first measurement) and 3.25 mm (second measurement) with standard deviations of 0.070 mm and 0.075 mm, respectively, when applying a force of at least 7 N. This results in compression factors of 0.76 and 0.78, respectively. This assumption was validated quantitatively by comparing the histograms of the soft tissue thicknesses measured by MRI and ultrasound, which shows a linear displacement (see Fig. 8). It is clear that after applying a correction factor to the MRI data, the histograms agree very well.

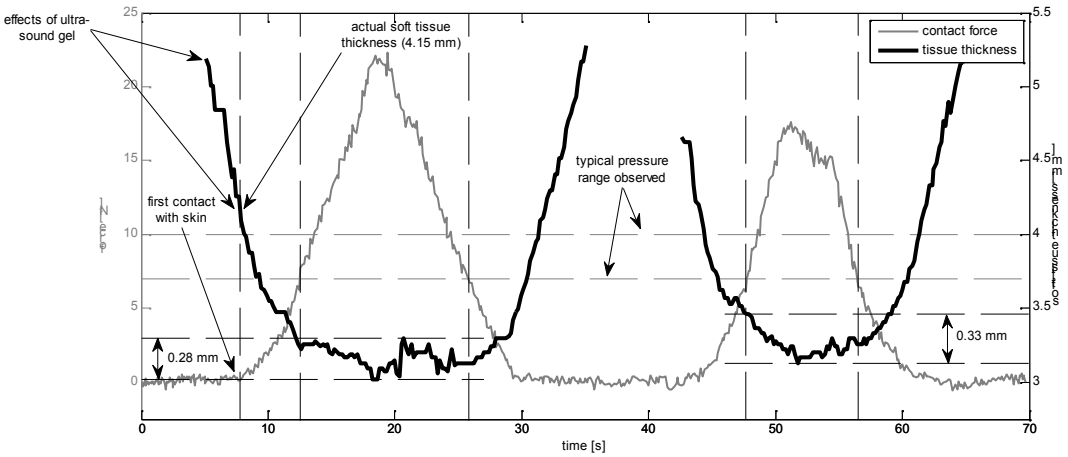

Fig. 7. Diagram of force applied to the subject's forehead (grey) and the measured soft tissue thickness (black). Gaps in the black graph indicate that no data was collected from the ultrasound probe (i.e. no contact). Also shown (dashed lines) are the range of typically used ultrasound force (7-10 N), first contact with the skin showing a thickness of 4.15 mm and the variation of measured tissue thickness for forces ≥ 7 N (0.28 mm and 0.33 mm).

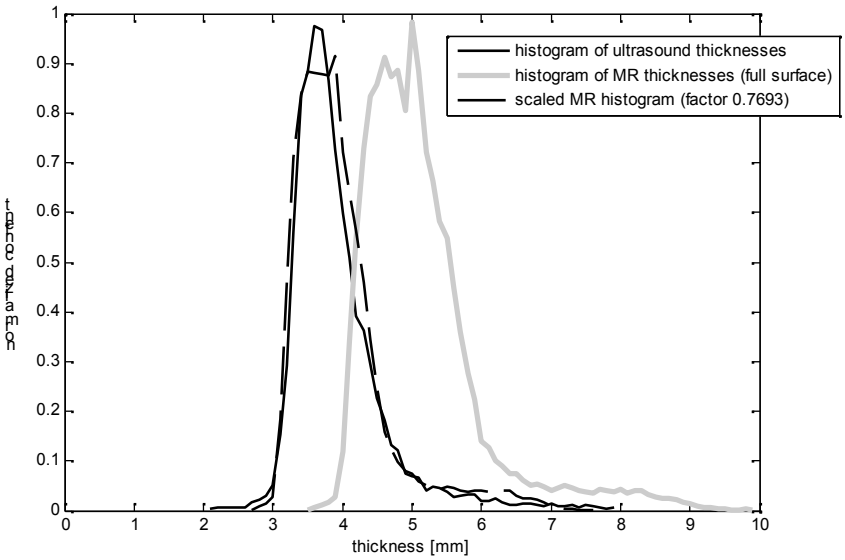

Fig. 8. Histograms of the soft tissue thickness as extracted from MRI (grey), from ultrasound (black) and when compensated (black dashed).

3.3 Thickness Comparison

The corrective factor determined in the force-compensated ultrasound setup was applied to the ultrasound data. The resulting thickness map is shown in Fig. 9. From visual inspection, this image shows features very similar to the map from Fig. 4(b).

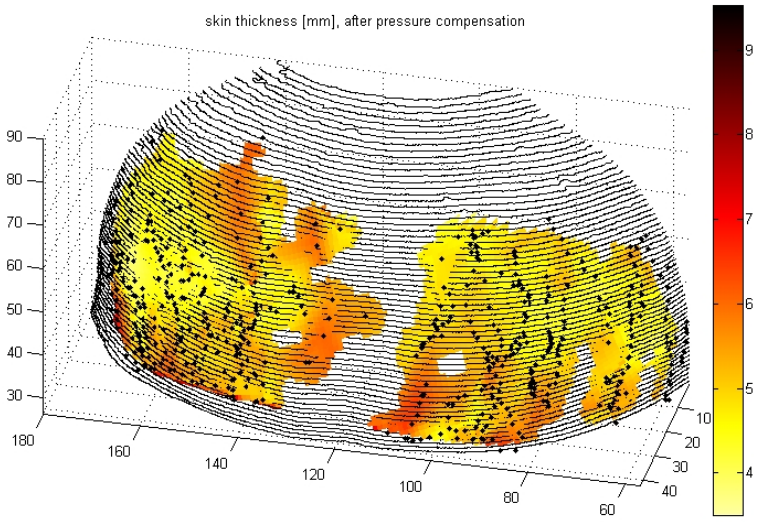

Fig. 9. Registration of the soft tissue estimated from ultrasound to the MRI data, compensated for transducer force

This data can now be compared to the thickness data obtained from MRI. For each sample of the ultrasound data, the closest sample from the MRI data was selected and the force-compensated soft tissue thickness from ultrasound was subtracted from the thickness estimated from the MRI scan. The results are given in Table 1.

Table 1. Statistics of the thickness errors

	Mean	Median	Std dev	Mean abs.	Max abs.
Error [mm]	0.1415	0.1048	0.8676	0.6314	3.6644

Clearly, although the mean value of the thickness error is relatively low (0.14 mm), several sources of measurement errors still influence the data. These are

- the limited resolution of the ultrasound data,
- the limited resolution of the MR data (voxel size 1 x 0.15 x 0.15 mm),
- possible segmentation errors in both the ultrasound and the MR data
- inaccuracies in the ICP registration, and
- errors from inaccurate correspondences in the registered data (the ultrasound thickness value is not measured at the same location as the closest MR thickness value).

4. CONCLUSION

We have shown that soft tissue thickness can be estimated from MR images as well as from tracked ultrasound. Using ICP-based registration and compensation for tissue compression, the thickness data agreed reasonably well.

With these measurements we could thus strengthen our hypothesis of the relation of the shift in the histogram and the contact force. This shows that ultrasound can constitute a valid ground truth for the proposed tracking system. Clearly, however, the study needs to be further expanded to determine the global applicability of the force compensation method. Influence of age, sex and individual conditions (including clinical conditions like oedema) may influence both the accuracy of the registration and the compressibility of the facial tissue.

ACKNOWLEDGEMENTS

Part of this work has been supported by Varian Medical Systems, Inc., and the German Federal Government's Excellence Initiative (grant number DFG GSC 235/1).

CONSENT

All authors declare that written informed consent was obtained from the test subjects for publication of this research article and accompanying images.

ETHICAL APPROVAL

The authors declare that the experiments were only performed as experiments on themselves. No other subjects were involved.

COMPETING INTERESTS

Authors have declared that no competing interests exist.

REFERENCES

1. Gill SS, Thomas DGT, Warrington AP, Brada M. Relocatable frame for stereotactic external beam radiotherapy. International Journal of Radiation Oncology, Biology, Physics. 1991;20:599–603. DOI: 10.1016/0360-3016(91)90076-g.

2. Norén G, Arndt J, Hindmarsh T, Hirsch A. Stereotactic Radiosurgical treatment of acoustic neurinomas. In: Lunsford LD, ed. Modern stereotactic neurosurgery. Vol 1. Topics in neurological surgery. Springer US; 1988:481–489. DOI: 10.1007/978-1-4613-1081-5_38.
3. Fuss M, Salter BJ, Cheek D, Sadeghi A, Hevezi JM, Herman TS. Repositioning accuracy of a commercially available thermoplastic mask system. Radiotherapy and Oncology. 2004;71:339–345. DOI: 10.1016/j.radonc.2004.03.003.
4. Tryggestad E, Christian M, Ford E, et al. Inter- and Intrafraction Patient Positioning Uncertainties for Intracranial Radiotherapy: A study of four frameless, thermoplastic mask-based immobilization strategies using daily cone-beam CT. International Journal of Radiation Oncology, Biology, Physics. 2011;80:281–290.DOI: 10.1016/j.ijrobp.2010.06.022.
5. Kooy HM, Dunbar SF, Tarbell NJ, Mannarino, E, Ferarro, N, Shusterman, S, Bellerive, M, Finn, L, McDonough, CV, Loeffler, JS. Adaptation and verification of the relocatable Gill-Thomas-Cosman frame in stereotactic radiotherapy. International Journal of Radiation Oncology, Biology, Physics. 1994;30:685–691. DOI: 10.1016/0360-3016(92)90956-i.
6. Ernst F, Bruder R, Wissel T, Stüber P, Wagner B, Schweikard A. Real time contact-free and non-invasive tracking of the human skull—first light and initial validation. In: Applications of Digital Image Processing XXXVI. San Diego, CA: Proceedings of SPIE vol. 8856; 2013:88561G-1–88561G-8. DOI: 10.1117/12.2024851.
7. Richter L, Bruder R. Design, implementation and evaluation of an independent real-time safety layer for medical robotic systems using a force-torque-acceleration (FTA) sensor. International Journal of Computer Assisted Radiology and Surgery. 2013;8:429–436. DOI: 10.1007/s11548-012-0791-5.
8. Besl PJ, McKay HD. A method for registration of 3-D shapes. IEEE Transactions on Pattern Analysis and Machine Intelligence. 1992;14:239–256. DOI: 10.1109/34.121791.
9. Chen Y, Medioni G. Object modeling by registration of multiple range images. In: Proceedings of the IEEE International Conference on Robotics and Automation. 1991:2724–2729. DOI: 10.1109/robot.1991.132043.

Peer-review history:
The peer review history for this paper can be accessed here:
http://www.sciencedomain.org/review-history.php?iid=311&id=12&aid=2397